Synthesis and Characterization of Nano MnFe₂O₄@CS@SO₃H for the Synthesis of Oxazolidin-2-one Derivatives

Fariba Heidarizadeh* & Farangis Sistani

Department of Chemistry, College of Science, Shahid Chamran University of Ahvaz, Ahvaz, Iran

*Corresponding author: heidarizadeh@scu.ac.ir (F. Heidarizadeh)

**ABSTRACT**

This project highlights the significance of oxazolidin-2-ones, a vital class of five-membered heterocyclic compounds renowned for their medicinal properties and uses as chiral auxiliary compounds. To facilitate the synthesis of oxazolidin-2-one derivatives, a novel approach employing acidic nanoparticles was employed. Specifically, a magnetic solid acid catalyst comprising sulfonic acid, stabilized on manganese ferrite nanoparticles with a chitosan coating (MnFe₂O₄@CS@SO₃H), was meticulously developed and characterized through various techniques. These nanoparticles exhibit remarkable thermal stability and can be effortlessly isolated from the reaction medium using a magnetic field owing to their inherent magnetic properties. Notably, analysis of FE-SEM images reveals the nanoparticles' uniform and spherical morphology, with a size scale in the nanometer range. This innovative catalyst promises to significantly enhance the efficiency of oxazolidin-2-one derivatives synthesis in chemical and pharmaceutical industries.
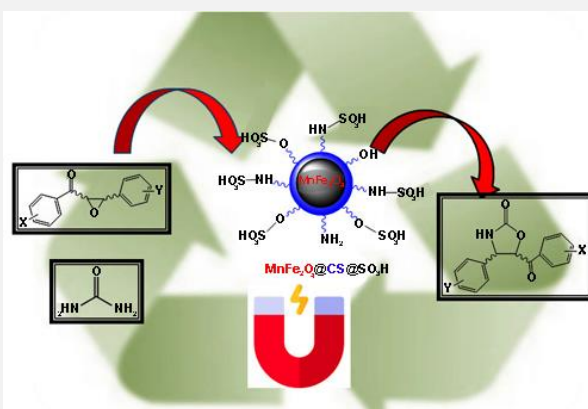
Keywords: Acid catalyst, carbamate, medicinal chemistry, nanocatalyst, oxazolidin-2-one derivatives

1. Introduction

Oxazolidin-2-ones, a class of five-membered heterocyclic compounds, play a pivotal role in medicinal chemistry and organic synthesis due to their diverse pharmacological activities and utility as essential components in drug development [1, 2]. Furthermore, their inherent chirality makes them particularly valuable for asymmetric synthesis, enabling the creation of enantiomerically pure compounds with high selectivity. However, traditional methods for synthesizing oxazolidin-2-one derivatives have historically presented challenges [3-5]. These methods often involve complex, multi-step processes, leading to intricacy and time-consuming procedures, ultimately reducing overall yields and increasing production costs. Achieving the necessary enantiomeric purity in chiral oxazolidin-2-one synthesis can be arduous, often necessitating costly and intricate chiral auxiliary groups or catalysts, which can introduce complexity and hinder scalability. Additionally, these historical routes frequently generate significant byproducts and waste, raising environmental concerns and complicating waste management. Some traditional methods also involve hazardous reagents or generate unstable intermediates, posing safety risks in laboratory and industrial settings. Furthermore, these approaches may exhibit low atom economy, where a substantial portion of starting materials is wasted, affecting resource efficiency and cost-effectiveness.

Scalability issues have historically presented challenges, as laboratory-developed methods may not readily transition to large-scale production due to difficulties related to heat and mass transfer and safety considerations. The choice of solvents in oxazolidin-2-one synthesis has also been a critical consideration, with some solvents being environmentally unfriendly or posing health risks, necessitating careful selection. Given these historical challenges, this study introduces an innovative approach to synthesizing oxazolidin-2-one derivatives. The groundbreaking method involves a magnetic solid acid catalyst stabilizing sulfonic acid on manganese ferrite nanoparticles with a

chitosan coating (MnFe$_2$O$_4$@CS@SO$_3$H). This catalyst possesses exceptional thermal stability, ensuring robust performance under various reaction conditions[3-6].

A remarkable feature of this catalyst is its magnetic property, allowing easy separation from the reaction medium by applying a magnetic field, streamlining the synthesis process, and reducing waste, aligning with the principles of green chemistry. Comprehensive characterization of MnFe$_2$O$_4$@CS@SO$_3$H using various techniques offers valuable insights into its structure and properties, with FE-SEM images confirming its nearly uniform, spherical morphology at the nanometer scale. In summary, the development of MnFe$_2$O$_4$@CS@SO$_3$H represents a significant advancement in the field of catalysis. It holds broad implications for the efficient, eco-friendly production of valuable oxazolidin-2-one derivatives, ultimately benefiting the pharmaceutical and chemical industries. However, it is imperative to remain attentive to historical and emerging challenges while advancing this field.

2. Materials and methods
2.1. Materials

The chemicals used in this research were purchased from Merck and Sigma Aldrich. The progress of the reaction was observed using thin-layer chromatography (TLC). Infrared spectra were recorded by FT-IR device BOMEM model, MB-series 1998, by KBr tablet in the 400-4000 cm^{-1} range. An ultrasonic bath model SONICA, 2200ETH S3, was used to disperse insoluble particles in solvents. The X-ray diffraction patterns of prepared nanoparticles were recorded by BRUKER, D8Advance device. FE-SEM images of the catalyst were recorded by MIRA III, TESCAN device. EDX elemental analysis and a map of the catalyst prepared by MIRA II, TESCAN, and MIRA III, TESCAN devices were performed. The magnetic properties of the studied materials were measured using the VSM device of Magnatis Daneshpajoh Kashan company. The thermal stability of the synthesized catalysts was investigated using TGA model STA 503/Bahr with a heating rate of 10 ˚C/min and in the temperature range of 20 to 1000 ˚C, and the surface area and voids of nanoparticles (BET) were determined by Micromeritics device.

2.2. Experimental
2.2.1. General method of synthesis of α-epoxy ketones

α-Epoxy ketones was synthesized according to our previous work[7].

2.2.2. Synthesis of manganese ferrite nanoparticles (MnFe$_2$O$_4$)

In a 250 mL Erlenmeyer flask, 10 mmol (1.69 g) of manganese sulfate monohydrate and 20 mmol (8 g) of iron (III) nitrate monahydrate were poured, and 100 mL of deionized water was added and stirred. 32 mL sodium hydroxide (3 M) solution was slowly added as a precipitating agent until the pH of the solution reached 10. Then, it was placed in an oil bath at 100 °C for 2 hours to prepare magnetic manganese ferrite nanoparticles. After the completion of the reaction, the nanoparticles were separated using a magnet, washed several times with deionized water and ethanol to remove impurities, and dried at 80 °C for 12 hours.

2.2.3. Synthesis of manganese ferrite nanoparticles with chitosan coating (MnFe$_2$O$_4$@CS) [8]

In a 250 mL Erlenmeyer flask, 0.5 g of chitosan was first dissolved in 50 mL of 2% acetic acid solution. Then, an ultrasonic bath added 0.5 grams of manganese ferrite and dispersed in the solution. 2.5 mL of 25% glutaraldehyde solution was added dropwise. After that, 1M sodium hydroxide solution was added dropwise until the pH of the solution reached 11. Then, it was heated for 12 hours at 40 °C, and after this period, it was washed with deionized water to neutralize the pH of the solution. The obtained product was dried overnight in an oven at 80 °C.

2.2.4. Synthesis of magnetic solid acid catalyst MnFe$_2$O$_4$@CS@SO$_3$H [9]

0.5 g of MnFe$_2$O$_4$@CS and 5.7 g of p-toluene sulfonic acid were added to 100 mL of ethanol and stirred for 24 hours at room temperature. The obtained product was washed several times with ethanol and dried overnight in an oven at 80 °C. The catalyst that was obtained is called MnFe$_2$O$_4$@CS@SO$_3$H (**Figure 1**).

2.2.5. Determination of acid strength of MnFe₂O₄@CS@SO₃H catalyst

To evaluate the acid strength of the MnFe$_2$O$_4$@CS@SO$_3$H catalyst, 100 mg of the catalyst was added to 25 mL of sodium chloride solution (pH=5.7, 1 M) in a beaker, and the prepared mixture was stirred for 24 hours until the pH of the solution It was reduced to 3.23. This decrease is equal to 0.146 mmol H$^+$/g cat.

2.2.6. General method for the synthesis of oxazolidin-2-one derivatives from the reaction of α-epoxy ketone derivatives and urea in the vicinity of the magnetic solid acid catalyst MnFe₂O₄@CS@SO₃H

In a 25 mL round-bottomed flask, 1 mmol of α-epoxy ketone derivative was dissolved in ethanol (5 mL), and 0.05 g of MnFe$_2$O$_4$@CS@SO$_3$H catalyst was added. Then, 1.5 mmol (0.09 g) of urea was added, and the reaction mixture was stirred at 60 °C on a magnetic stirrer. TLC monitored the progress of the reaction in a solvent mixture of n-hexane: ethyl acetate (1:5). After the completion of the reaction, the catalyst was separated using a magnet. The solution was concentrated at 50 °C to produce the crude product. Then, the crude product was isolated and purified through thin-layer chromatography on a silica gel GF254 60 plate (n-hexane: ethyl acetate, 1:5) (reaction 1).

3. Results and discussion

The MnFe$_2$O$_4$@CS@SO$_3$H catalyst emerges as a crucial player in catalysis, amalgamating distinctive features that elevate its importance in diverse chemical processes. Incorporating manganese and iron within the catalyst imparts magnetic properties and bestows it with catalytic prowess in redox reactions. Chitosan, serving as the intermediate layer, not only provides structural integrity but also introduces environmentally friendly aspects owing to its biodegradability and abundance. Incorporating sulfonic acid groups (SO$_3$H) further enhances the catalyst's functionality, facilitating strong acidic sites that catalyze various organic transformations. This tripartite composition synergistically combines magnetic responsiveness, biocompatibility, and acidic reactivity, making MnFe$_2$O$_4$@CS@SO$_3$H a versatile catalyst with applications in green chemistry, sustainable synthesis, and the production of valuable compounds with reduced environmental impact. Its significance lies in its ability to contribute to catalytic processes' efficiency and environmental sustainability (**Figure 1**).
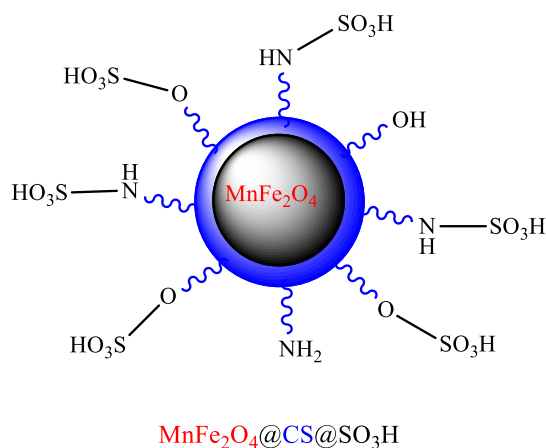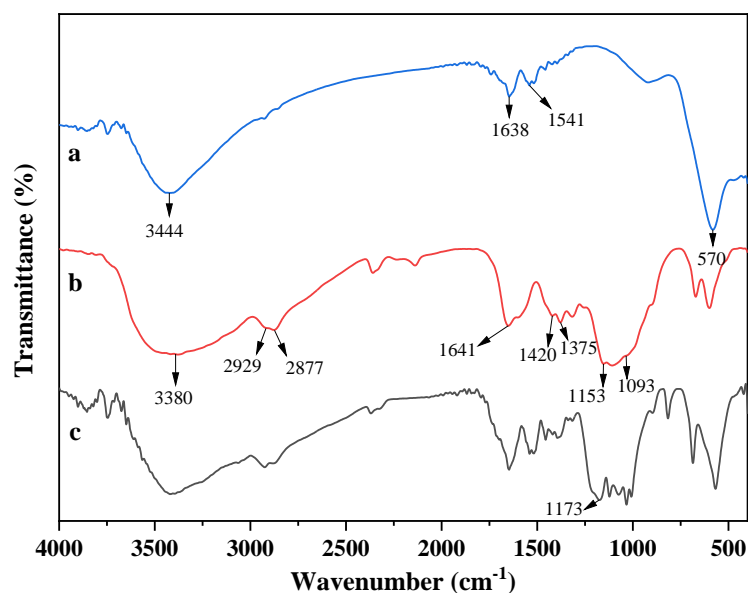

MnFe$_2$O$_4$@CS@SO$_3$H

Figure 1. MnFe₂O₄@CS@SO₃H structure.

In this catalyst, Glutaraldehyde serves as a cross-linking agent. It contains aldehyde functional groups that can react with amino groups present in chitosan. This reaction forms covalent bonds between chitosan molecules, creating a stable, cross-linked structure. The reaction between glutaraldehyde and chitosan helps stabilize the chitosan coating on the surface of the magnetic nanoparticles. This stabilization is crucial for maintaining the integrity of the coating during subsequent steps and under various conditions. The stable chitosan coating, achieved through glutaraldehyde cross-linking, contributes to the overall performance of the catalyst. It helps maintain the active sites of the sulfonic acid groups on the surface of the nanoparticles, ensuring efficient catalysis during reactions.

3.1. Identification of MnFe$_2$O$_4$@CS@SO$_3$H catalyst

The structural characteristics of acid catalysts were identified and investigated using FT-IR, FE-SEM, XRD, EDX, VSM, TGA, and BET methods.

FT-IR spectrum of three compounds, MnFe$_2$O$_4$, chitosan, and MnFe$_2$O$_4$@CS@SO$_3$H, can be seen in **Figure 2**. The peaks that appeared in the region of 570 cm^{-1} in the MnFe$_2$O$_4$ spectrum are attributed to the stretching vibrations of the Fe-O and Mn-O bonds in the tetrahedral and octahedral cavities in the spinel structure, which confirms that the prepared sample has a spinel structure [10]. The observed peak at 3444 cm^{-1} is attributed to the symmetric stretching vibrations of O-H groups, and the peaks at 1638 and 1541 cm^{-1} are attributed to the symmetric stretching vibrations of hydrogen bonds (H-O-H) of surface water molecules, indicating the presence of adsorbed or free water in the sample [11]. According to the chitosan spectrum, characteristic peaks of chitosan functional groups can be observed. The peak appearing in the region of 3380 cm^{-1} is related to the stretching vibrations of N-H and O-H bonds. The absorption peaks in the 2929 and 2877 cm^{-1} region can be attributed to the stretching vibrations of the C-H bond. The stretching vibrations of the C=O group of the amide and the C-O group appear at the wavelength of 1641 and 1093 cm^{-1}, respectively, and the asymmetric stretching vibrations of the C-O-C groups of the polysaccharide structure are observed in the region of 1153 cm^{-1}. Also, the peaks related to CH$_2$ bending vibrations were located at 1420 and 1375 cm^{-1} [12]. FT-IR spectrum of MnFe$_2$O$_4$@CS@SO$_3$H also shows a peak in the region of 1173 cm^{-1}, which can be attributed to the symmetric and asymmetric O=S=O stretching vibrations of SO$_3$H groups [13].

Figure 2. FTIR of (**a**) MnFe$_2$O$_4$,(**b**) chitosan , and (**c**) MnFe$_2$O$_4$@CS@SO$_3$H

The X-ray diffraction (XRD) pattern of manganese ferrite nanoparticles is shown in **Figure 3**, which is in good agreement with JCPDS standard card 00-010-0319. This pattern has six sharp peaks at angles 2θ = 29.87, 35.10, 42.69, 52.64, 56.36, 61.83, respectively, which correspond to crystal plates (220), (311), (400), (422), (511), (440) structure of manganese ferrite is related and confirms its cubic spinel structure. Chitosan coating did not change the MnFe$_2$O$_4$ indicator peaks. In addition, a very weak and broad peak is observed at the angle 2θ=14-25˚, related to the amorphous structure of chitosan polymer [14, 15].
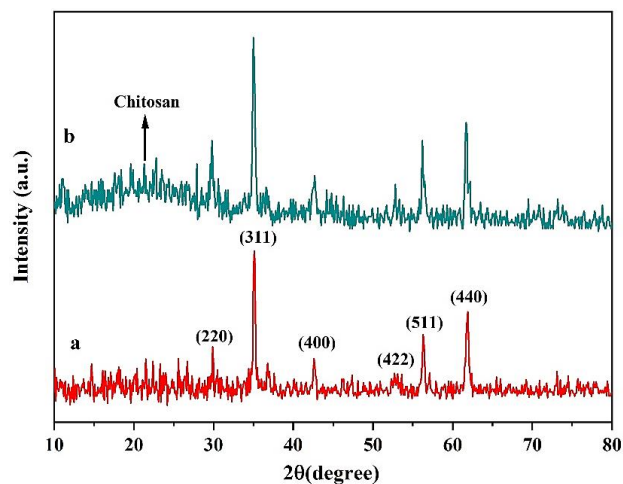
Figure 3. XRD pattern of (**a**) $MnFe_2O_4$ (**b**) $MnFe_2O_4@CS@SO_3H$

According to the FE-SEM images, the nanoparticles have spherical and almost uniform shapes, and the size of $MnFe_2O_4@CS@SO_3H$ particles is about 41-49 nm. In addition, placing the chitosan coating on the surface of manganese ferrite nanoparticles has caused changes in its surface structure and morphology (**Figure 4**).
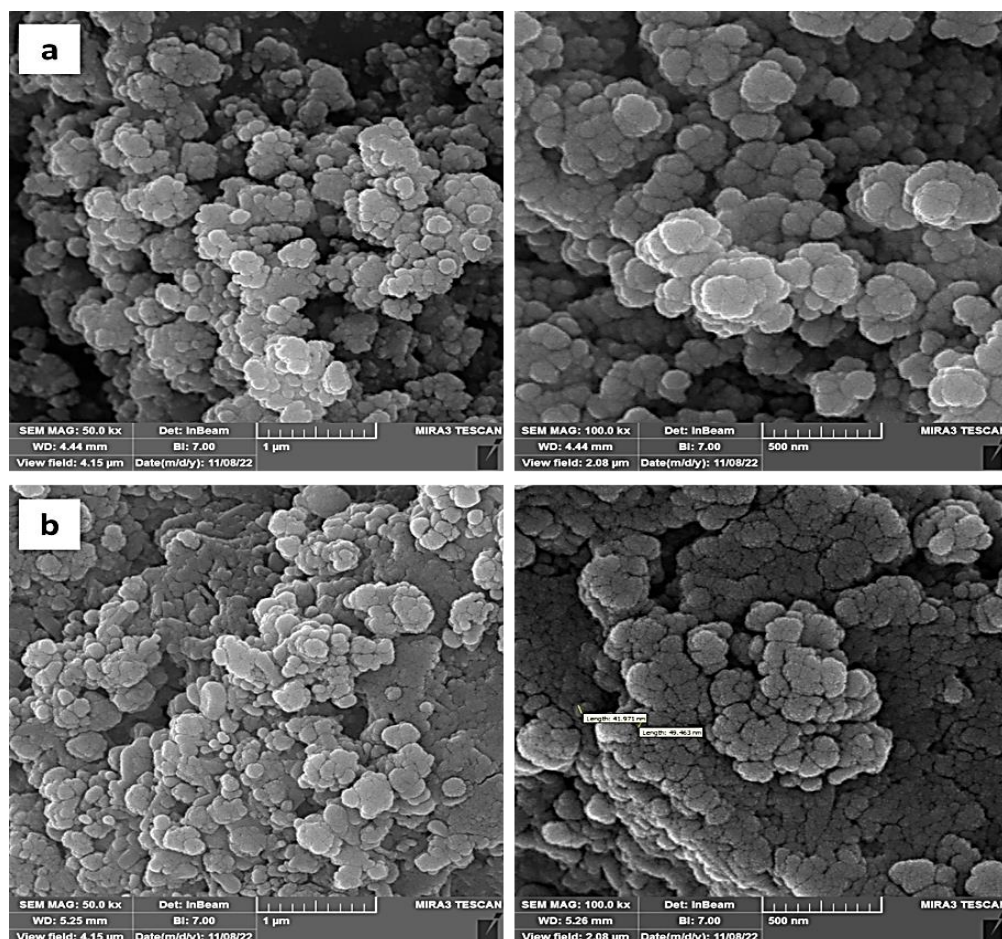

Figure 4. FESEM of (**a**) $MnFe_2O_4$ (**b**) $MnFe_2O_4@CS@SO_3H$

X-ray energy diffraction spectroscopy (EDX) related to $MnFe_2O_4@CS@SO_3H$ catalyst, except for hydrogen, all the elements in the composition, including manganese, iron, nitrogen, oxygen, carbon, and sulfur, are present. Therefore, it can be concluded that the sulfonic acid functional group is placed on the surface of manganese ferrite nanoparticles with chitosan coating (**Figure 5**). The mapping images show the uniform distribution of Fe, Mn, O, N, C, and Si atoms (**Figure 6**).
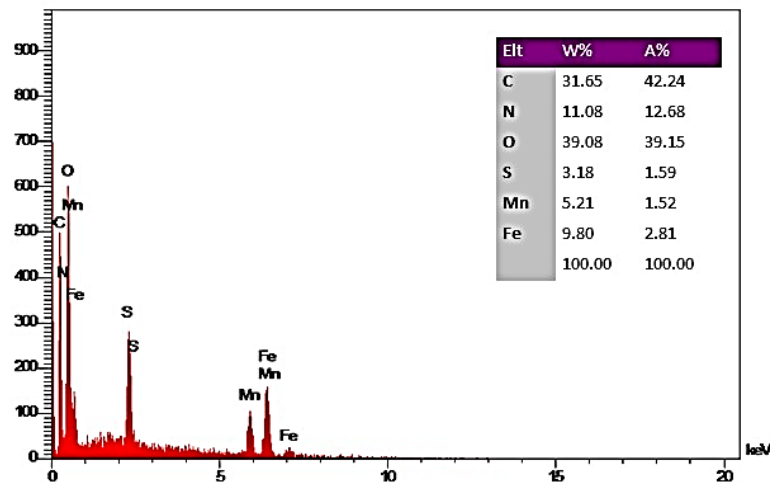
Elt	W%	A%
C	31.65	42.24
N	11.08	12.68
O	39.08	39.15
S	3.18	1.59
Mn	5.21	1.52
Fe	9.80	2.81
	100.00	100.00

Figure 5. EDX of $MnFe_2O_4@CS@SO_3H$
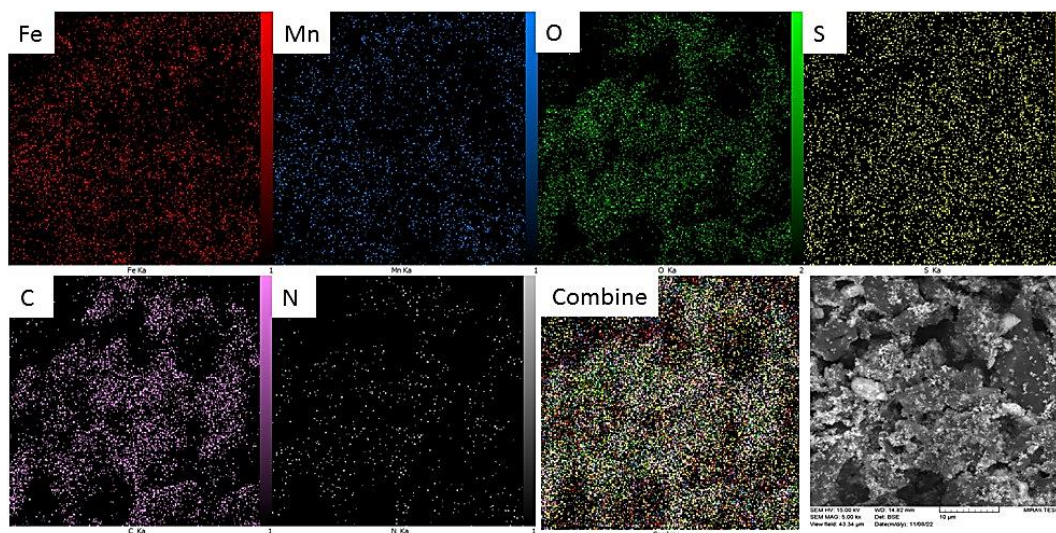
Figure 6. Mapping analysis of $MnFe_2O_4@CS@SO_3H$.

The magnetic properties of $MnFe_2O_4$ and $MnFe_2O_4@CS@SO_3H$ nanoparticles were measured by vibrating sample magnetometer (VSM) analysis under a magnetic field with a strength of 15 kOe at ambient temperature. The magnetic saturation value (Ms) for $MnFe_2O_4$ and $MnFe_2O_4@CS@SO_3H$ equals 52.64 and 12.14 emu/g, respectively (**Figure 7**). The decrease in the magnetic saturation of the nanocatalyst compared to the manganese ferrite is due to the non-magnetic chitosan multilayer coating on the $MnFe_2O_4$ magnetic cores. This multi-layer coating reduces the mutual effects of the magnetic cores by avoiding their proximity to each other. Despite the decrease in magnetization, this nanocatalyst can still be separated from the reaction medium by an external magnet.
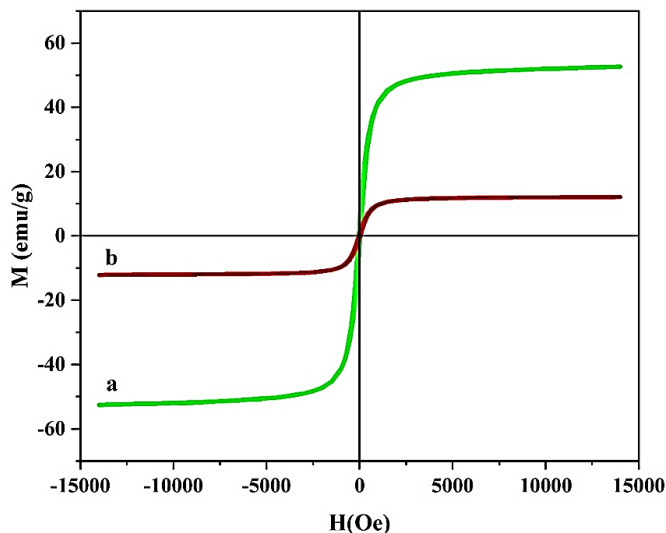
Figure 7. VSM curve of (**a**) $MnFe_2O_4$, (**b**) $MnFe_2O_4@CS@SO_3H$

Thermal gravimetric analysis (TGA) is used to check the stability of the sample against heat. The TGA curve shows three stages of mass reduction of $MnFe_2O_4@CS@SO_3H$ (**Figure 8**). The first stage of weight loss occurs in the temperature range of 50-320 ˚C with the loss of 5.54 mg of mass, which can be related to the loss of small molecules such as network water molecules or solvents in the structure of the catalyst. In the second stage, a mass reduction of 11.56 mg was observed in the temperature range of 320-650 ˚C, which is related to the decomposition of cross-linked amine and hydroxyl groups in the chitosan polymer structure, and in the third stage, a 0.97 mg decrease in the mass of the sample was observed in the range of ˚C 650-1000 is related to the decomposition of chitosan residues. The results show that the $MnFe_2O_4@CS@SO_3H$ catalyst has good stability up to 320 ˚C, and its decomposition occurs at higher temperatures [7].
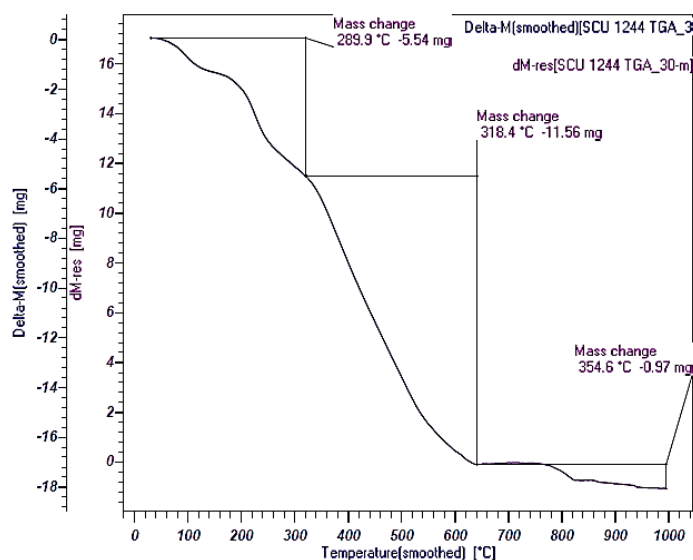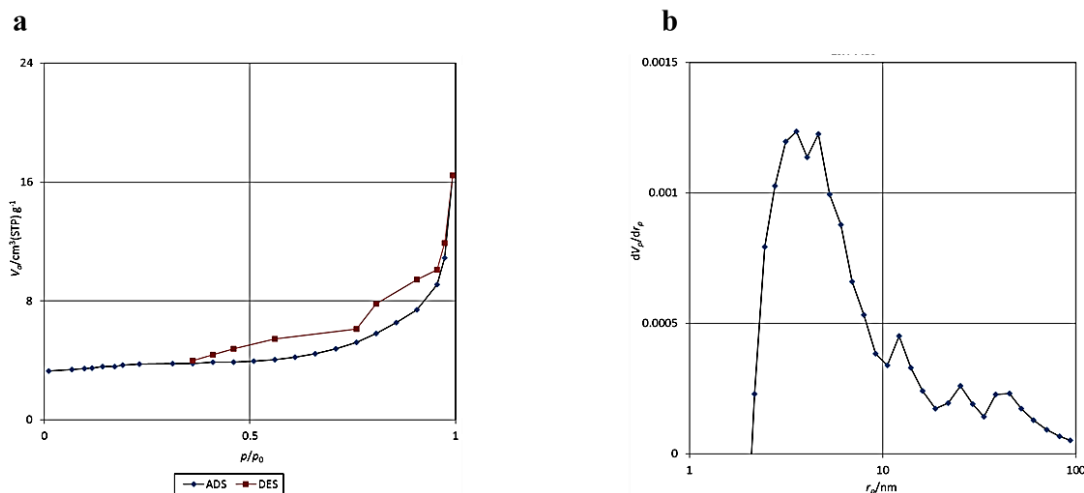

Figure 8. TGA of $MnFe_2O_4@CS@SO_3H$

Figure 9 shows the results of measuring the surface area, average particle size, porosity, and hole size based on measuring the volume of nitrogen gas absorbed and desorbed by the material's surface at a temperature of 77 K. The specific surface area of the composition is equal to 13.43 m^2/g. The reason for the low specific surface area can be attributed to the magnetic property of the catalyst. This is because the magnetic nanoparticles stick to each other, and

the contact surface for the adsorbed gas is reduced. The diameter of the holes in $MnFe_2O_4@CS@SO_3H$ nanoparticles is equal to 1.7 nm. As a result, a mesoporous structure can be considered for this compound. Also, the radius and volume of the cavity are equal to 3.58 nm and 0.019 cm^3/g, respectively.

a   **b**

Figure 9. Nitrogen adsorption-desorption isotherm plots of (**a**) $MnFe_2O_4@CS@SO_3H$ and (**b**) BJH pore distribution of $MnFe_2O_4@CS@SO_3H$

3.2. Optimizing reaction conditions for the synthesis of oxazolidin-2-one derivatives in the presence of $MnFe_2O_4@CS@SO_3H$ catalyst

The reaction of alpha-epoxyketone (**Scheme 1**) and urea in the vicinity of different amounts of $MnFe_2O_4@CS@SO_3H$ catalyst in different solvents and temperatures was investigated to determine the optimal conditions. The amount of catalyst plays an essential role in increasing the speed and efficiency of the reaction. The reaction did not take place within 24 hours in the absence of the catalyst (**Table 1**). An increase in efficiency was observed by increasing the amount of catalyst from 0.01 to 0.06 grams. Amounts greater than 0.05 grams of catalyst did not change the reaction efficiency. Therefore, the optimal amount of catalyst used was determined to be 0.05 g. Investigating the effect of the solvent in the reaction showed that the reaction was not performed after 24 hours in any of the solvents. Water, dichloromethane, dimethyl sulfoxide, acetonitrile, ethyl acetate, and Ethanol were the only suitable solvents for the reaction. The effect of temperature on the progress of the reaction showed that the reaction did not occur at ambient temperature after 24 hours, but with increasing temperature, an increase in the reaction efficiency was observed. However, a rise above 60 ˚C did not show a significant change in yield. The results show that the optimal conditions for performing the reaction per 0.05 g of $MnFe_2O_4@CS@SO_3H$ catalyst are in ethanol solvent and at 60 ˚C.
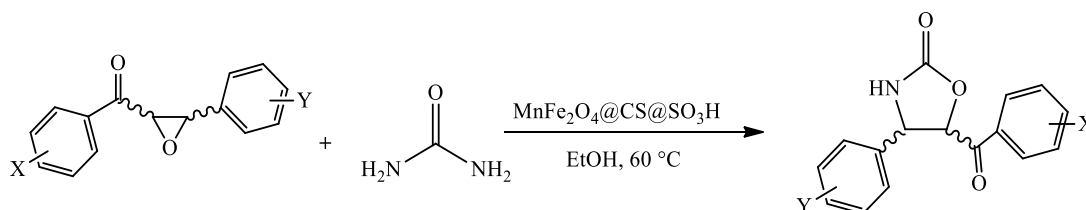
Scheme 1. Synthesis of oxazolidin-2-one derivatives in the presence of $MnFe_2O_4@CS@SO_3H$

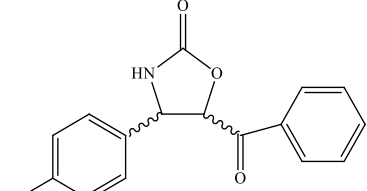**Table 1.** Optimization of oxazolidin-2-one synthesis in the presence of MnFe$_2$O$_4$@CS@SO$_3$H
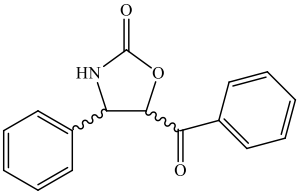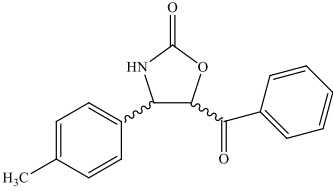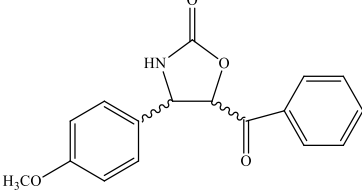
Entry	Amount of catalyst (g)	T(°C)	Solvent	Time (h)	Yield^a (%)
1	0.05	60	CH$_2$Cl$_2$	24	—
2	0.05	60	CH$_3$CN	24	—
3	0.05	60	EtOAc	24	—
4	0.05	60	DMSO	24	—
5	0.05	60	H$_2$O	24	—
6	—	60	EtOH	24	—
7	0.05	70	EtOH	2	78
8	0.05	60	EtOH	2.1	79
9	0.05	50	EtOH	3	75
10	0.05	25	EtOH	24	—
11	0.06	60	EtOH	2.1	79
12	0.04	60	EtOH	3.1	70
13	0.03	60	EtOH	4	62
14	0.02	60	EtOH	6	57
15	0.01	60	EtOH	8	50
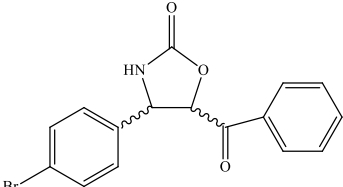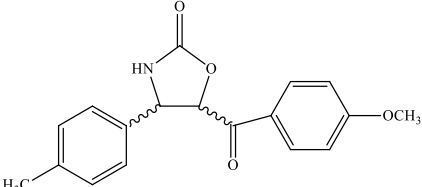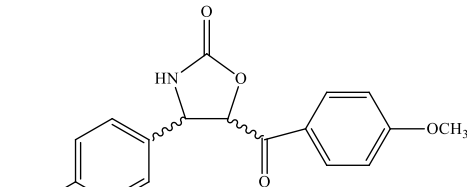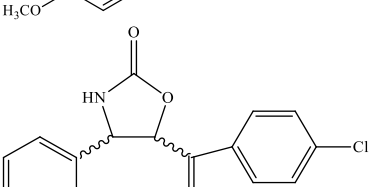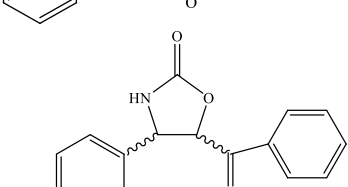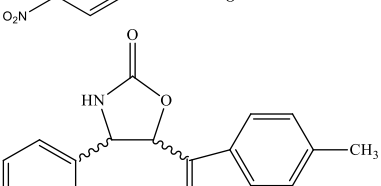
^{a}Isoated yield

3.3. Preparation of oxazolidin-2-one derivatives in the presence of MnFe$_2$O$_4$@CS@SO$_3$H catalyst

After determining the optimal conditions, the reaction of α-epoxyketone derivatives (1a-k, **Table 2**) with urea was investigated in the presence of MnFe$_2$O$_4$@CS@SO$_3$H catalyst, and disubstituted 4,5-oxazolidin-2-one derivatives were synthesized (**Table 2**). The products were characterized using FT-IR and melting point analysis, and their characteristics were compared with those of known samples.

Table 2. Oxazolidin-2-one derivatives prepared in the presence of MnFe$_2$O$_4$@CS@SO$_3$H^a

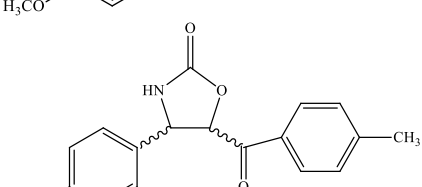| Entry	α-epoxy ketone	Product	Time (min)	Yield^b (%)
1	**1a**		**130**	**79**
2	**1b**		**90**	**86**
3	**1c**		**100**	**80**
4	**1d**		**170**	**60**

5	1e		150	65

6	1f		95	75

7	1g		110	72

8	1h		110	76

9	1i		120	68

10	1j		h 24	—

11	1k		130	70

[a] α-Epoxy ketone (1 mmol), $MnFe_2O_4$@CS@SO_3H catalyst (0.05 g), and urea (1.5 mmol, 0.09 g) in ethanol (5 mL) at 60 °C.
[b] Isolated yield

3.4. Reaction mechanism of the synthesis of oxazolidin-2-one derivatives

The proposed reaction mechanism is shown in **Figure 10**. First, by the nucleophilic attack of one of the urea nitrogens on C_β of the epoxide ring in the presence of the acidic catalyst $MnFe_2O_4$@CS@SO_3H while H^+ helps to loosen the bond between oxygen and C_β, transition state 1 is formed. Further, the opening of the epoxide ring leads to the formation of intermediate 2. After the rotation of intermediate 2 around the C_α-C_β bond, the attack of oxygen on the carbonyl group carbon, and the removal of NH_3, the compound is rapidly cyclized, and 4,5-disubstituted

oxazolidin-2-one derivatives are formed. Electron donating groups such as CH_3, through the induction effect by increasing the electron density on the Ar' ring, and OCH_3 group due to having a non-bonding electron pair through resonance, cause more stability of the transition state and increase the speed and efficiency of the reaction.

On the other hand, electron-withdrawing groups such as Br and Cl reduce the stability of the transition state by causing adverse induction effects. This slows the reaction rate because stability barriers increase and the mechanism does not proceed optimally. The NO_2 group is a strong electron withdrawer, and due to its ability to absorb electrons and create resonance effects, it is very effective in terms of induction and electrons. This group provides enough stability in the C_β-oxygen bond that the C-O bond does not break easily, and the transition state does not form quickly. This causes no reaction in this situation. The presence of electron-donating and electron-withdrawing groups on the Ar ring also does not significantly affect the progress of the reaction due to the significant distance from the reaction center. Therefore, it can be concluded that the type and position of electron groups in molecules significantly affect the reaction's speed and efficiency.
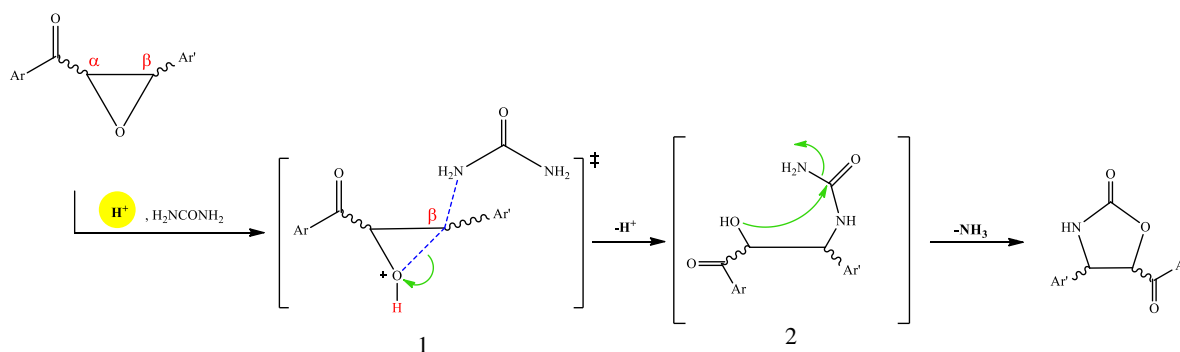
Figure 10. Reaction mechanism of alpha epoxy ketone derivatives and urea in the presence of acid catalyst $MnFe_2O_4@CS@SO_3H$

4. Evaluating the synthesis of oxazolidine-2-ones in comparison to methods documented in existing literature

To demonstrate the efficacy of this catalyst in the reaction involving α-epoxy ketone derivatives and urea, the outcomes from this study were compared with findings from other sources (**Table 3**). It is crucial to underscore the limited existing literature on synthesizing oxazolidine-2-ones from chalcones, underscoring the necessity for additional investigations in this domain. $MnFe_2O_4@CS@SO_3H$ emerges as a practical and versatile catalyst sharing comparable magnetic properties.

Table 3. Comparison of the synthesis of Oxazolidine-2-ones with methods described in the literature

Entry	Catalyst (amount)	Reaction conditions	Time	Yield (%)	Ref.
1	$MnFe_2O_4@CS$-PTA (3 mg)	EtOH- 60 ℃	90 min	89	[7]
2	PTSA 0.1 mmol (0.0172 g)	DMF 60-70 ℃	5h	82	[16]
3	$MnFe_2O_4@CS@SO_3H$ (5 mg)	EtOH- 70 ℃	130 min	79	This work

5. Conclusions

In this project, a solid magnetic sulfonic acid catalyst stabilized on chitosan-coated manganese ferrite nanoparticles ($MnFe_2O_4@CS@SO_3H$) was prepared and successfully reacted with alpha-epoxyketone derivatives with urea to prepare oxazolidin-2-one derivatives. Having suitable magnetic power, easy separation of the catalyst using an external magnetic field, high thermal stability, short time, and relatively high reaction efficiency are the advantages of using this catalyst. The novelty of this work stems from the combination of a unique catalyst design, innovative use of acidic nanoparticles, thorough characterization techniques, practical features like magnetic isolation, and the potential impact on the synthesis of oxazolidin-2-one derivatives in relevant industries. Finally, Evaluating the

environmental effect of the catalyst and the reaction is essential to ensure sustainability and minimize the environmental footprint of the synthesis process. Investigating the catalyst's potential in other organic synthesis reactions could open up new avenues for its application. Finally, transferring the technology to industry for commercialization would allow for widespread adoption of this innovative catalyst, making its benefits accessible to a broader audience. Moreover, the catalysts' recyclability enhances their desirability for various applications, enabling cost-effective and environmentally friendly processes.

Authors' contributions

All authors contributed to data analysis, drafting, and revising of the paper and agreed to be responsible for all aspects of this work.

Declaration of competing interest

The authors declare no competing interest.

Funding

This paper received funding with grant no.1400.

Data availability

Data will be made available on request.

References

[1] X. You, K.-W. Hu, H. Zong, X. Wen, H. Yuan, K. Cheng, Q.-L. Xu, Z. Lai, Synthesis of polycyclic fused oxazolidin-2-ones by catalytic Boron (III)-Promoted oxo-Michael addition reaction and evaluation on their cytotoxicity, Tetrahedron 149(2023) 133714.

[2] M.R. Sarfjoo, A. Shad, M. Hassanpour, R.S. Varma, An Overview on New Anticancer Drugs Approved by Food and Drug Administration: Impending Economic and Environmental Challenges. Mater. Chem. Horizons, 1(2022), 189-198.

[3] B. Maleki, O. Reiser, E. Esmaeilnezhad, H.J. Choi, SO_3H-dendrimer functionalized magnetic nanoparticles ($Fe_3O_4@$ DNH (CH_2) $4SO_3H$): Synthesis, characterization and its application as a novel and heterogeneous catalyst for the one-pot synthesis of polyfunctionalized pyrans and polyhydroquinolines, Polyhedron 162 (2019) 129-141.

[4] F. Adibian, A.R. Pourali, B. Maleki, M. Baghayeri, A. Amiri, One-pot synthesis of dihydro-1H-indeno [1, 2-b] pyridines and tetrahydrobenzo [b] pyran derivatives using a new and efficient nanocomposite catalyst based on N-butylsulfonate-functionalized MMWCNTs-D-NH_2, Polyhedron 175 (2020) 114179.

[5] S.S. Karbasaki, G. Bagherzade, B. Maleki, M. Ghani, Magnetic $Fe_3O_4@$ SiO_2core–shell nanoparticles functionalized with sulfamic acid polyamidoamine (PAMAM) dendrimer for the multicomponent synthesis of polyhydroquinolines and dihydro-1H-indeno [1, 2-b] pyridines, Org. Prep. Proced. Int. 53(5) (2021) 498-508.

[6] S.S. Karbasaki, G. Bagherzade, B. Maleki, M. Ghani, Fabrication of sulfamic acid functionalized magnetic nanoparticles with denderimeric linkers and its application for microextraction purposes, one-pot preparation of pyrans pigments and removal of malachite green, J. Taiwan. Inst. Chem. Eng. 118 (2021) 342-354.

[7] R. Mozafari, F. Heidarizadeh, F. Nikpour, $MnFe_2O_4$ magnetic nanoparticles modified with chitosan polymeric and phosphotungstic acid as a novel and highly effective green nanocatalyst for regio-and stereoselective synthesis of functionalized oxazolidin-2-ones, Mater. Sci. Eng. C 105 (2019) 110109.

[8] Y. Zhang, Y. Wang, Z. Zhang, W. Cui, X. Zhang, S. Wang, Removing copper and cadmium from water and sediment by magnetic microspheres-MnFe2O4/chitosan prepared by waste shrimp shells, J. Environ. Chem. Eng. 9(1) (2021) 104647.

[9] A. Wang, H. Li, H. Pan, H. Zhang, F. Xu, Z. Yu, S. Yang, Efficient and green production of biodiesel catalyzed by recyclable biomass-derived magnetic acids, Fuel Process. Technol. 181 (2018) 259-267.

[10] S. Kanagesan, S.B.A. Aziz, M. Hashim, I. Ismail, S. Tamilselvan, N.B.B.M. Alitheen, M.K. Swamy, B. Purna Chandra Rao, Synthesis, characterization and in vitro evaluation of manganese ferrite (MnFe2O4) nanoparticles for their biocompatibility with murine breast cancer cells (4T1), Molecules 21(3) (2016) 312.

[11] K.H. Liew, T.K. Lee, M.A. Yarmo, K.S. Loh, A.F. Peixoto, C. Freire, R.M. Yusop, Ruthenium supported on ionically cross-linked chitosan-carrageenan hybrid MnFe2O4 catalysts for 4-nitrophenol reduction, Catalysts 9(3) (2019) 254.

[12] A. Drabczyk, S. Kudłacik-Kramarczyk, M. Głąb, M. Kędzierska, A. Jaromin, D. Mierzwiński, B. Tyliszczak, Physicochemical investigations of chitosan-based hydrogels containing Aloe vera designed for biomedical use, Materials 13(14) (2020) 3073.

[13] I. Elsayed, M. Mashaly, F. Eltaweel, M.A. Jackson, Dehydration of glucose to 5-hydroxymethylfurfural by a core-shell $Fe_3O_4@$ SiO_2-SO_3H magnetic nanoparticle catalyst, Fuel 221 (2018) 407-416.

[14] M.M. Baig, M.A. Yousuf, P.O. Agboola, M.A. Khan, I. Shakir, M.F. Warsi, Optimization of different wet chemical routes and phase evolution studies of $MnFe_2O_4$ nanoparticles, Ceram. Int. 45(10) (2019) 12682-12690.

[15] P.R. Thombal, S.S. Han, Novel synthesis of Lewis and Bronsted acid sites incorporated CS-Fe3O4@ SO3H catalyst and its application in one-pot synthesis of tri (furyl) methane under aqueous media, Biofuel Res. J. 5(4) (2018) 886-893.

[16] F. Nikpour, S. Mohebbi, T. Paibast, M. Beigvand, Regio-and stereoselective synthesis of functionalized oxazolidin-2-ones from the reaction of α-epoxyketones with urea, Monatsh. Chem. 139 (2008) 663-667.